The Novel Tubulin-Binding Checkpoint Activator BAL101553 Inhibits EB1-Dependent Migration and Invasion and Promotes Differentiation of Glioblastoma Stem-like Cells

Raphael Berges, Aurelie Tchoghandjian, Stéphane Honore, Marie-Anne A Estève, Dominique Figarella-Branger, Felix Bachmann, Heidi A Lane, Diane Braguer

The Novel Tubulin-Binding Checkpoint Activator BAL101553 Inhibits EB1-Dependent Migration and Invasion and Promotes Differentiation of Glioblastoma Stem-like Cells

Raphaël Bergès[1], Aurélie Tchoghandjian[1], Stéphane Honoré[1,2], Marie-Anne Estève[1,2], Dominique Figarella-Branger[1,2], Felix Bachmann[3], Heidi A. Lane[3], and Diane Braguer[1,2]

Abstract

Glioblastoma patients have limited treatment options. Cancer stem-like cells (CSLC) contribute to glioblastoma invasiveness and repopulation; hence, they represent promising targets for novel therapies. BAL101553 is a prodrug of BAL27862, a novel microtubule-destabilizing agent inhibiting tumor cell proliferation through activation of the spindle assembly checkpoint, which is currently in phase I/II clinical development. Broad anticancer activity has been demonstrated against human cancer models, including tumors refractory to conventional treatments. We have shown that overexpression of microtubule + end-binding 1-protein (EB1) correlates with glioblastoma progression and poor survival. Here, we show that BAL27862 inhibits the growth of two glioblastoma CSLCs. As EB1 is overexpressed in the CSLC line GBM6, which displays a high tumorigenicity and infiltrative pattern of migration *in vivo*, we investigated drug activity on GBM6 according to EB1 expression. BAL27862 inhibited migration and colony formation at subcytotoxic concentrations in EB1-expressing control cells (GBM6-sh0) but only at cytotoxic concentrations in EB1-downregulated (GBM-shE1) cells. Three administrations of BAL101553 were sufficient to provoke an EB1-dependent survival benefit in tumor-bearing mice. Patterns of invasion and quantification of tumor cells in brain demonstrated that GBM6-sh0 cells were more invasive than GBM6-shEB1 cells, and that the antiproliferative and anti-invasive effects of BAL101553 were more potent in mice bearing control tumors than in EB1-downregulated tumors. This was associated with inhibition of stem cell properties in the GBM6-sh0 model. Finally, BAL27862 triggered astrocytic differentiation of GBM6 in an EB1-dependent manner. These results support the potential of BAL101553 for glioblastoma treatment, with EB1 expression as a predictive biomarker of response. *Mol Cancer Ther; 15(11); 2740–9. ©2016 AACR.*

Introduction

Glioblastomas are the most aggressive brain tumors in adults (1). Despite progress, effective therapies are limited, especially at the time of relapse. The aggressiveness of glioblastoma resides in their high proliferation rate and invasive behavior, making complete tumor resection impossible. Therefore, targeting these invasive cells could help improve current therapies (2). A hallmark characteristic of glioblastoma is their functional cellular heterogeneity (3), and the existence of a small population of cancer stem-like cells (CSLC) described to be at the origin of the tumor and to drive relapses due to their capacity of self-renewal and resistance to chemo- and radiotherapy (4–7). Furthermore, experimental data clearly show that glioblastoma CSLCs are responsible for glioblastoma invasiveness (8). The identification of CSLCs in brain tumors provides a powerful tool to investigate the development of malignancies and to develop therapies targeting these cells. Another approach to tackle CSLCs resides in the induction of differentiation to suppress their stem cell properties and tumorigenic potential.

Microtubule-targeting agents (MTA) are a very successful class of cancer drugs with therapeutic benefits in diverse cancers (9). Despite this, resistance to currently approved MTAs does occur, modulated by P-gp overexpression or tubulin and/or apoptotic pathway protein modifications (10). The use of MTAs for glioblastoma treatment is restricted due to the blood–brain barrier that blocks the crossing of most of the clinically relevant, natural product-derived MTAs into the brain (11). BAL27862 is a novel small molecule MTA that was discovered by optimization of high-throughput screening hits. The compound binds to the colchicine site with distinct effects on microtubule (MT) organization (12, 13). It is a very potent inhibitor of tumor cell growth and promoter of cell death, whose activity is associated with activation of the spindle assembly checkpoint (14). Moreover, BAL27862 retains its antiproliferative activity in human tumor models resistant to clinically relevant MTAs (binding the taxane or the *Vinca*-alkaloid site on tubulin) as a result of diverse resistance mechanisms (15, 16). Furthermore, the drug demonstrates cytotoxic effects in glioblastoma cell lines and, in animal models, is

[1]Aix Marseille Univ, INSERM, CRO2 UMR911, Marseille, France. [2]APHM, CHU Timone, Marseille, France. [3]Basilea Pharmaceutica International Ltd., Basel, Switzerland.

Note: Supplementary data for this article are available at Molecular Cancer Therapeutics Online (http://mct.aacrjournals.org/).

Corresponding Authors: Diane Braguer, Aix-Marseille University, Pharmacy Faculty, 27 bd Jean Moulin, 13385 Marseille Cedex05, France. Phone: 33-491-835635; E-mail: diane.braguer@univ-amu.fr; and Heidi A. Lane, Basilea Pharmaceutica International AG, Grenzacherstrasse 487, Postfach, 4005 Basel, Switzerland. Phone: 41-61-606-11-11; E-mail: heidi.lane@basilea.com

doi: 10.1158/1535-7163.MCT-16-0252

efficiently distributed into the brain and the tumor (17). BAL101553, a highly soluble prodrug of BAL27862, is currently undergoing clinical evaluation in advanced cancer patients by i.v. (phase IIA) or oral (phase I) administration (18–20). Previously, we reported that microtubule + End-binding 1-protein (EB1) was a factor of bad prognosis in glioblastoma, and that *Vinca*-alkaloid chemotherapy could improve the treatment of glioblastoma patients with an EB1-overexpressing tumor (21). We demonstrated notably the EB1-dependent migratory potential of two human primary glioblastoma CSLCs, GBM6 and GBM9, established from sorted $A2B5^+$ cells (22). GBM6 and GBM9 represent two appropriate study models of glioblastoma (i.e., mesenchymal and proneural, respectively) that displayed specific molecular signatures and strikingly differed in their *in vitro* and *in vivo* behavior (23).

Here, we investigated the activity of BAL27862 and its prodrug BAL101553 on glioblastoma CSLCs according to EB1 expression level *in vitro* and in orthotopically transplanted nude mice, respectively. We demonstrated that BAL27862 is the first MTA able to inhibit glioblastoma CSLCs proliferation and migration *in vitro* in an EB1-dependent manner. Moreover, three intravenous BAL101553 administrations over the course of a week were sufficient to provoke a significant and EB1-dependent survival benefit in tumor-bearing mice, together with a decrease in tumor growth and brain invasion. Interestingly, drug treatment triggered astrocytic differentiation of glioblastoma CSLCs in an EB1-dependent manner. By demonstrating for the first time a novel role of an MTA in promoting differentiation of glioblastoma CSLCs, these findings provide new insights into the anticancer properties of the investigational drug BAL101553, with important implications for the therapeutic targeting of glioblastoma CSLCs.

Materials and Methods

Cell lines and reagents

We used two human primary glioblastoma stem cell lines, GBM6 and GBM9, previously established from two different human glioblastoma tumor samples and characterized in our laboratory (22, 23). They represent two appropriate study models of glioblastoma that differed in their cellular composition, displayed specific molecular signatures and strikingly differed in their *in vitro* behavior. Indeed, GBM6 cells were highly migratory whereas GBM9 cells exhibited much lower migratory capacities but a higher proliferation rate. GBM6 and GBM9 were used at passages 92 and 104, respectively. Cells were grown in serum-free medium supplemented with EGF and bFGF as previously described (22).

BAL27862 and BAL101553 (Supplementary Fig. S1) were provided by Basilea Pharmaceutica International Ltd (Basel, Switzerland). BAL27862 is the active moiety of the lysine prodrug BAL101553, which was developed to improve solubility and allow i.v. application in saline solutions without the need for solubilizing excipients associated with unwanted side effects (e.g., cremophor). Hence, the prodrug BAL101553 was used for all animal experiments. As the cleavage of the prodrug BAL101553 is incomplete in cell culture medium, the active moiety BAL27862 was used for *in vitro* assessments.

Cell transfections

ShRNA plasmid that specifically knocked out human EB1 (NM_012325) and negative shRNA control plasmid (Mission non-target shRNA control vector) were obtained from Sigma-Aldrich. Cells were transfected according to the protocol previously described (21). Stable GFP-shRNA–transfected cells were obtained after transfection with peGFP-N3 vector (Clontech) using lipofectamineTM 2000 system (Invitrogen) and selection with 0.6 mg/mL geneticin (Life Technologies).

Cytotoxic assay

Cells (5,000 cells/well) were seeded on poly-DL-ornithine (Sigma-Aldrich) coated 96-well plates (10 μg/mL) and allowed to grow for 24 hours before treatment with BAL27862. Growth inhibition of cells was measured after 72 hours by using a sulforhodamine B assay kit (Sigma-Aldrich) as described previously (21).

Clonogenic survival assay

Cells were grown on poly-DL-ornithine coated 6-well plates (1000 cells/well) and after a 72 hours treatment with BAL27862, incubated for up to 5 days. Colonies were stained with 1% crystal-violet solution in 20% methanol (Sigma-Aldrich). The colonies with more than 50 cells were counted.

Cell migration assay

CSLCs (50,000 per condition) were poured on the upper side of a transwell migration chamber (0.8 μm filter, BD) in DMEM. The lower side of the chamber was filled with DMEM, supplemented with 10% FCS. Cell migration was quantified as described (21).

Cell invasion assay

Cells were mixed with 1.7 mg/mL fluorescein (FITC)-conjugated collagen type I (Invitrogen) solution and seeded in a 48-well plate at the density of 10^6 cells/mL. After polymerization of collagen, phenol red-free DMEM medium containing BAL27862 was added for 48 hours. Invasion was assessed using a microplate reader (Polarstar omega, BMG Labtech).

In vitro FACS analysis

For analysis of BAL27862 prodifferentiating effects, cells were seeded at 300,000 cells/well. One day later, cells were treated with BAL27862 for 72 hours. Then, cells were trypsinized and incubated with A2B5-APC antibody (clone 105HB29, reference 130-093-582; Miltenyi Biotec). Cells were then fixed and analyzed using flow cytometry (FACS Calibur, BD Biosciences). A total of 100,000 events were counted for each sample, and data were recorded with the CellQuest Pro Software (BD Biosciences) and analyzed using FlowJo software (Tree Star Inc.) choosing the Dean-Jet-Fox model analysis.

For the neural lineage analysis, cells were fixed and permeabilized, then sequentially incubated with antibodies (anti-CNPase-FITC, 1/500, Abcam; anti-β-III-tubulin-Alexa 647, 1/20, BD Pharmingen; and GFAP-PE, 1/500, BD Pharmingen) and processed for analysis.

Self-renewal capacity determination

The effect of BAL27862 on self-renewal capacity on glioblastoma stem cells was evaluated by limiting dilution. GBM6 cells were seeded in poly-DL-ornithine coated 6-well plates (150,000 cells/well). After 24 hours, cells were treated with or without BAL27862 for 72 hours. The supernatant was then removed, and cells were harvested, dissociated into single cells and plated

in 96-well plates (1–5 cells/well). Eight days later, the spheres were counted under an inverted light microscope (Leica DMI 4000B) (Leica). Sphere formation efficiency was calculated as the number of spheres formed divided by the original number of cells seeded (24). Three independent experiments were performed.

RNA extraction

Total RNA was extracted using QIAamp RNA Blot Mini kit (Qiagen) according to the manufacturer's instructions. RNA samples with no evidence of ribosomal peak degradation and RIN values of 6 to 10 were used for real-time quantitative PCR analyses (25) after treatment with 1 U ribonuclease-free deoxyribonuclease (Roche Applied Science) at 37°C for 15 minutes (Supplementary data and Supplementary Table S1).

Animal experiments

All experimental procedures and animal care were carried out in conformity with the guidelines of the French Government and approved by the Regional Committee for Ethics on Animal Experiments (authorization number 0100903). Six- to 8-week-old female athymic nude mice were obtained from Harlan Laboratories France. Using a stereotaxic frame (Kopf), about 100,000 cells of GBM6-GFP-sh0 or shEB1 cells were stereotactically injected into the subventricular zone (0.5 mm anterior to bregma, −1 mm lateral, and −2.1 mm deep to the cortex surface), as previously described (23). Four groups ($n = 8$) were constituted for GBM6-GFP-sh0 and GBM6-GFP-shEB1 bearing mice, respectively, receiving BAL101553 intravenously at 30, 33, and 36 days after glioma implantation (25 mg/kg in 5 mL/kg application volume) or vehicle solution (5 mL/kg, control groups). At 45, 75, and 105 days after glioma implantation, three animals of each group were sacrificed for analysis of tumor volumes by 3D reconstruction (23) or for FACS analysis (Supplementary data).

Statistical analysis

Data are presented as mean ± SEM. At least, three independent experiments were performed for each condition in cellular studies. Cell counting and cellular viability data were analyzed by the Student t test. Survival medians were estimated by the Kaplan–Meier product limit method. The log-rank test was used to compare survival rates by univariate analysis. Reported P values are two-sided, and $P < 0.05$ was considered statistically significant. Asterisks indicate significant level versus control: *, $P < 0.05$; **, $P < 0.005$; ***, $P < 0.001$. Statistical analyses were performed with GraphPad 5.0 statistical software.

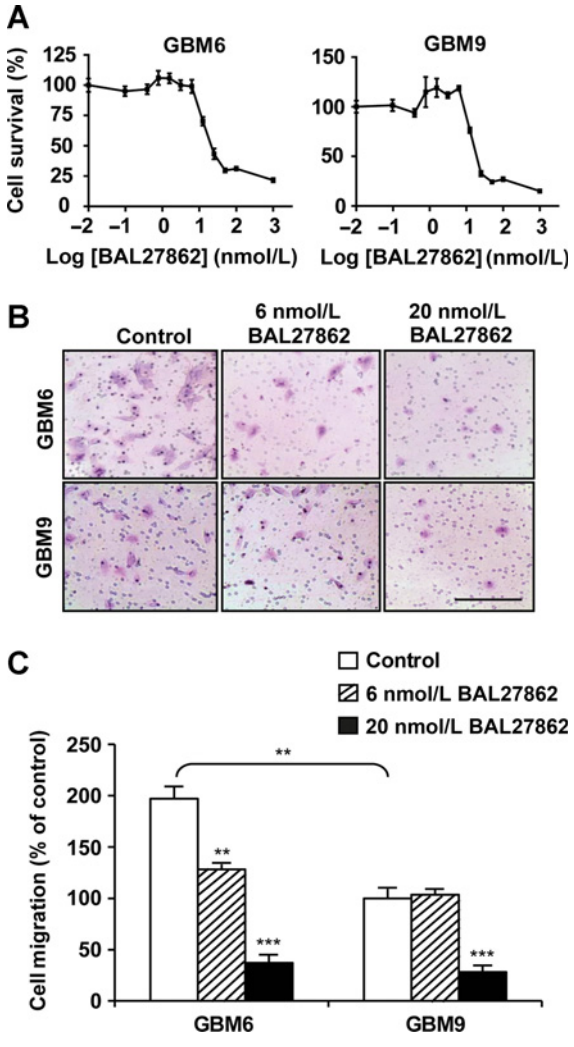

Figure 1.
BAL27862 inhibits growth and migration of glioblastoma stem-like cells. **A,** dose–response curves of the cytotoxicity of BAL27862 in GBM6 and GBM9. **B,** representative images of GBM6 and GBM9 migratory cells treated or not (control) with BAL27862 using the Transwell migration assay. Bar, 200 μm. **C,** quantification of migratory cells treated or not with BAL27862. Quantification was expressed as a percentage of migrating cells relative to 100% of control cells. Bar ± SEM. **, $P < 0.005$; ***, $P < 0.001$.

Results

BAL27862 inhibits growth and migration of glioblastoma stem-like cells

BAL27862 treatment was investigated on two human primary glioblastoma CSLCs, GBM6 and GBM9. Cells were treated with 0 to 1,000 nmol/L for 3 days (Fig. 1A). BAL27862 dose-dependently exerted cytotoxic activity on both glioblastoma CSLCs lines at low nanomolar concentrations ($EC_{50} = 20.8 \pm 1.3$ nmol/L and 21.7 ± 0.8 nmol/L for GBM6 and GBM9, respectively). For subsequent experiments, we used 3 to 10 nmol/L and 20 nmol/L BAL27862 as noncytotoxic and cytotoxic concentrations, respectively. BAL27862 exposure also affected the capacity of glioblastoma CSLCs to migrate, as assessed using the transwell migration assay (Fig. 1B and 1C). As expected with an MTA, the cytotoxic concentration (20 nmol/L) drastically inhibited the migration of both CSLC lines. However, at the noncytotoxic concentration (6 nmol/L), GBM6 cells showed a statistically significant inhibition of cell migration, whereas GBM9 cells did not respond. Because GBM6 overexpress EB1 as compared with GBM9 (20), we then investigated whether the high expression of EB1 sensitizes GBM6 CSLCs to the anti-migratory effect of BAL27862.

EB1 expression potentiates BAL27862 antimigratory and anticlonogenic effects on glioblastoma stem-like cells

For deciphering how EB1 influences GBM6 cell response to BAL27862 treatment, we generated both transitory and

stable clones deficient for EB1 (GBM6-siEB1 and GBM6-shEB1; Supplementary Fig. S2). Typical comet-like staining of EB1 was observed in GBM6-wt and GBM6-si0 (Supplementary Fig. S2C). EB1 was barely visible in GBM6-siEB1 cells (Supplementary Fig. S2B and 2C). GBM6-shEB1 showed a 69% reduction of the EB1 expression level as compared with control sh0 or wt-GBM6 cells (Supplementary Fig. S2A). GBM6-shEB1 and GBM6-sh0 were also stably transfected with GFP, without modification of the relative EB1 expression levels (Supplementary Fig. S2A).

As we demonstrated previously that EB1 expression correlates with glioblastoma cell migration in U87-MG (20), we first investigated the role of EB1 expression in GBM6 using stable downregulation of EB1. The knockdown of EB1 expression in untreated cells significantly decreased cell migration (by 35.7% ± 4.9% for GBM6-GFP-shEB1 as compared with control GBM6-GFP-sh0, $P < 0.05$; Fig. 2A and 2B), confirming the promigratory role of EB1 in CSLCs as previously described in U87-MG (20). We next assessed the effect of EB1 expression on the antimigratory properties of BAL27862. BAL27862 inhibited GBM6-GFP-sh0 and GBM6-GFP-shEB1 cell migration. However, the noncytotoxic concentration (6 nmol/L) was efficient in control cells but not in GBM6-GFP-shEB1 cells. Similar results were obtained in control GBM6-si0 cells versus GBM6-siEB1 cells treated with 6 nmol/L BAL27862 (Fig. 2C and D).

We then tested whether BAL27862 could inhibit invasion of CSLCs cells by performing a collagen I degradation assay (Fig. 2E). Indeed, very low concentrations of BAL27862 (3 and 6 nmol/L) decreased invasion of the GBM6-sh0 cells but failed to inhibit invasion of GBM6-shEB1 cells. Furthermore, a clonogenic assay was performed to analyze the effect of 3, 6, and

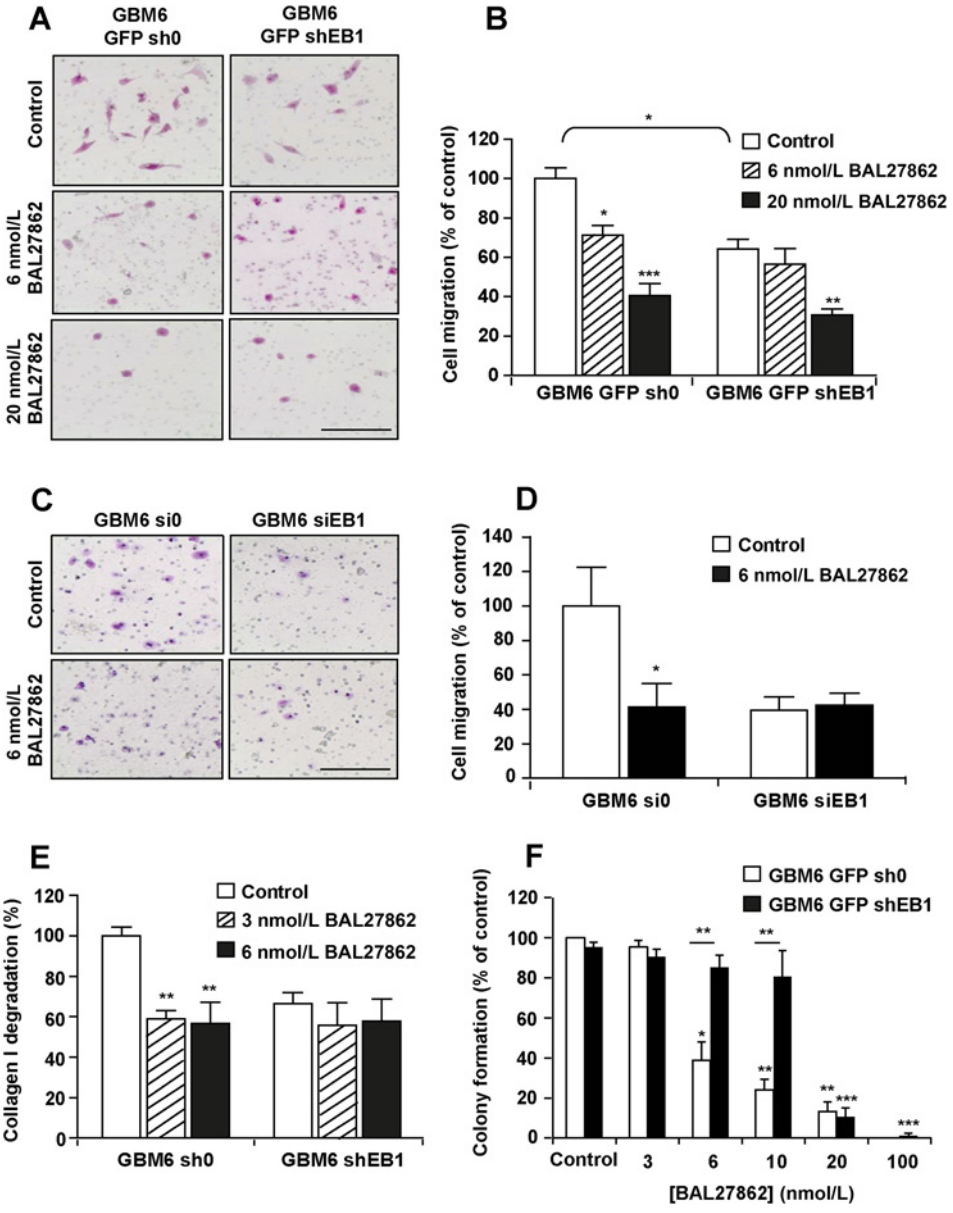

Figure 2.
EB1 expression potentiates BAL27862 antimigratory and anticlonogenic effects on glioblastoma stem-like cells. Representative images (**A**) and quantification (**B**) of EB1-downregulated GBM6 cells (GBM6-shEB1) or control GBM6-sh0 migratory cells treated or not (control) with BAL27862. Bar, 200 μm. Representative images (**C**) and quantification (**D**) of migratory GBM6 transfected with EB1-specific siRNA (GBM6-siEB1) or siRNA control (GBM6-si0), and treated or not with BAL27862. Bar, 200 μm. Quantification is expressed as a percentage of migrating cells relative to 100% of control cells. **E,** GBM6-sh0 or GBM6-shEB1 cells were cultivated for 48 hours in FITC-collagen containing BAL27862 or DMSO (control). Invasion was assessed by determining the amount of FITC released into the supernatant. **F,** colony-forming assay performed on GBM6-GFP-sh0 or GBM6-GFP-shEB1 treated or not with BAL27862 for 72 hours. The graph shows the number of colonies relative to 100% of GBM6-GFP-sh0 control cells. Bar, ± SEM. *, $P < 0.05$; **, $P < 0.005$; ***, $P < 0.001$.

10 nmol/L BAL27862 on GBM6 clonogenicity after 72 hours of exposure (Fig. 2F). Importantly, BAL27862 impaired the clonogenic capacity of GBM6 CSLCs at noncytotoxic concentrations in a statistically significant manner only in GBM-sh0 cells. Altogether, these results show that BAL27862 phenocopies the effect of EB1 knockdown on migration and clonogenicity in GBM6 cells.

BAL101553 treatment enhances survival and reduces tumor growth and invasion in mice orthotopically grafted with GBM6 cells

To investigate whether the EB1 expression level influences drug response also *in vivo*, control GBM6-GFP-sh0 or GBM6-GFP-shEB1 cells were transplanted by stereotaxy into the subventricular zone of nude mice at day 0, and animals were treated with 25 mg/kg BAL101553 (prodrug of BAL27862) i.v. or vehicle control at 30, 33, and 36 days. Survival and tumor analysis at 45, 75, and 105 days after grafting were then performed. A significant survival benefit was observed in the groups of animals treated with BAL101553, independent of the EB1 expression level (Fig. 3A and B). However, BAL101553 was more efficient if EB1 was not downregulated (survival gain of 37.5 days, $P < 0.05$). We then quantified GFP^+ tumor cells in the brain by FACS (Fig. 3C) and performed serial sagittal sections of brains to analyze migration patterns (Fig. 3D). Pictures taken from single sections were used for a 3D reconstruction of brains (23; see insets in Fig. 3D). GBM6-GFP-sh0 cells largely invaded the brain. Cells (green in the sections and corresponding 3D reconstruction) started to invade deeply the brain (Fig. 3D a) and, at a later stage, they migrated to the contralateral hemisphere by using the corpus callosum (gray in the 3D reconstructions) as a path (Fig. 3D i), as confirmed by the high number of fluorescent cells in the brain (1.7 ± 0.34 at day 105). In contrast, brain invasion was less pronounced in EB1 downregulated tumor grafted mice (0.68 ± 0.18, $P < 0.05$; Fig. 3C and 3D c, g, k), confirming the bad prognostic value of EB1 expression in glioblastoma (21). Hematoxylin/eosin coloration and Ki67 staining confirmed this observation (not shown). Importantly, BAL101553 treatment of GBM6-GFP-sh0 tumors resulted in a clear reduction of the tumor mass (size) (0.92 ± 0.08 vs. 1.7 ± 0.34 for vehicle-treated mice, $P < 0.05$; Fig. 3C) and in tumor spreading (Fig. 3D b, f, j), indicating a suppressive effect of BAL101553 on tumor growth and brain invasion *in vivo*. However, the effect of BAL101553 was minimal in GBM6-GFP-shEB1 tumors as compared with vehicle controls (0.73 ± 0.07 vs. 0.69 ± 0.18 for vehicle-treated mice; Fig. 3C and 3D d, h, l). These results are consistent with the *in vitro* data where EB1 expression positively correlates with BAL27862 activity on glioblastoma CSLCs (Figs. 1 and 2). Taken together, our results show that EB1 expression, despite its bad prognostic value, may be considered as a predictive marker for BAL101553 response.

BAL101553 induces loss of stem cell properties, potentiated by EB1 expression.

To decipher the mechanism of action of the drug, we first sorted by FACS GFP^+ tumor cells and then quantified $A2B5^+$ and $A2B5^-$ tumor cells 45, 75, and 105 days after grafting (Fig. 4A and B). At day 0, only $A2B5^+$ tumor cells were grafted. At day 45, BAL101553 treatment of GBM6-GFP-sh0 tumors shifted the proportion of tumor cells in favor of $A2B5^-$ cells which is a clear shift in comparison with the control. In contrast, in GBM6-GFP-shEB1 tumors, $A2B5^+$ cells remained the predominant cell population upon BAL101553 treatment, indicating a higher content of CSLCs in EB1 downregulated tumors as compared with EB1-expressing tumors at this time. However, a decrease in the proportion of $A2B5^+$ cells was detected in GBM6-GFP-shEB1 tumors later, at day 75. These results showed that BAL101553 treatment reduces the proportion of CSLCs in GBM6 orthotopic tumor-bearing mice, being particularly potent in EB1-expressing tumors. A complementary set of experiments were then performed *in vitro* with the active moiety BAL27862 to detail its effect on glioblastoma CSLCs. FACS analysis showed a significant decrease of $A2B5^+$ cells with the noncytotoxic concentration of BAL27862 (6 nmol/L, 72 hours) only in GBM6-GFP-sh0 cells (Fig. 4C). A higher cytotoxic concentration of BAL27862 (20 nmol/L) was active whatever the level of EB1 expression. Importantly, the decrease in $A2B5^+$ cells observed at 6 nmol/L was not due to apoptosis, as annexin V–positive staining was detectable only at 20 nmol/L (Fig. 4D).

A statistically significant decrease in sphere formation frequency was also observed in GBM6-GFP-sh0 cells treated with 6 nmol/L BAL27862 (Fig. 4E and F), whereas in GBM6-GFP-shEB1 cells, a statistically significant loss of capacity to form spheres was observed only at 20 nmol/L. This indicates that subcytotoxic concentrations of BAL27862 reduced the self-renewal potential of GBM6 CSLCs in an EB1 expression-dependent manner.

BAL27862 induces GBM6 astrocytic differentiation, potentiated by EB1 expression

As cellular differentiation is associated with typical morphological changes, we analyzed the morphology of GBM6 CSLCs after BAL27862 treatment. Interestingly, exposure to a low concentration of BAL27862 (6 nmol/L) triggered a significant increase in cell elongation and area of GBM6-GFP-sh0 cells, whereas it caused no phenotypic changes in GBM6-GFP-shEB1 (Fig. 5A and B). Together with the loss of A2B5 expression and a lower capacity for sphere formation, these data suggest that BAL27862 triggers differentiation of GBM6 CSLCs in an EB1 expression-dependent manner.

We next investigated whether BAL27862 regulates expression levels of neural differentiation markers. To this end, we focused on the three major lineages by analyzing astrocytic differentiation using GFAP expression, neuronal differentiation using β-III-tubulin expression and oligodendroglial differentiation using CNPase expression (Fig. 5C and D). Interestingly, BAL27862 significantly increased the amount of $GFAP^+$ cells and GFAP mRNA level in GBM6-sh0 at 6 and 20 nmol/L. In contrast, GFAP was increased only after exposure to the higher dose (20 nmol/L) in GBM6-shEB1 cells. Conversely, CNPase protein levels were decreased in GBM6-sh0 only after treatment with 20 nmol/L BAL27862, and no changes in β-III-tubulin protein and mRNA levels were found after BAL27862 treatment either in GBM6-sh0 or in GBM6-shEB1.

Discussion

In this study, we have performed detailed correlative analyses, both *in vitro* and in orthotopic tumors, providing proof of principle that microtubule disruption is a rationale therapeutic approach for targeting glioblastoma CSLCs. Using the novel MTA

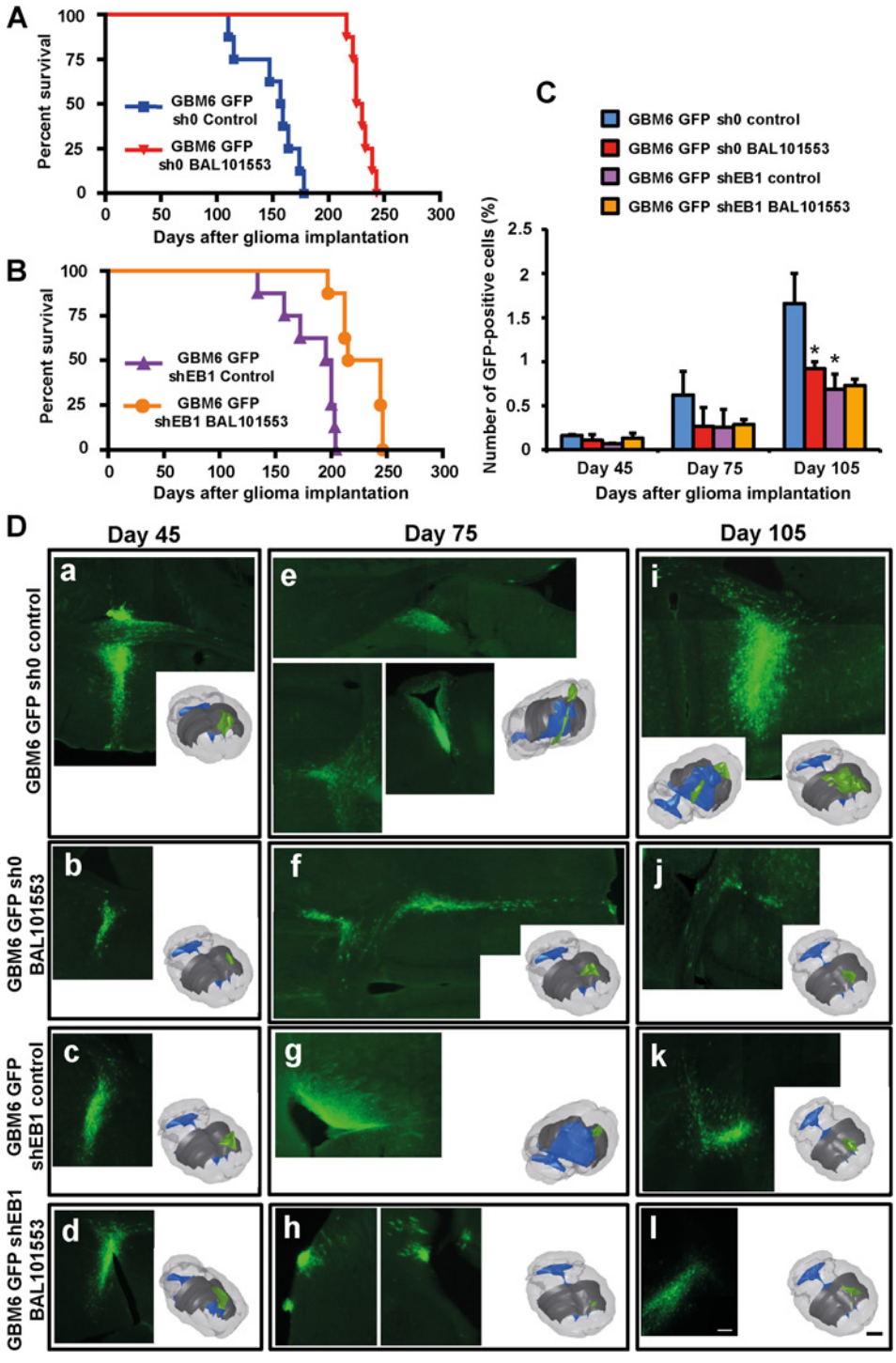

Figure 3.
BAL101553 treatment enhances survival and reduces tumor growth and brain invasion in mice orthotopically grafted with GBM6 cells. Kaplan–Meier survival plot of control GBM6-GFP-sh0 (**A**) or EB1-downregulated GBM6-GFP-shEB1 (**B**) bearing mice i.v. treated with BAL101553 (three times at 25 mg/kg) or vehicle (control). **C,** quantification by FACS analysis of tumor GFP-positive cells isolated from brains of mice grafted with control GBM6-GFP-sh0 or GBM6-GFP-shEB1 treated with BAL101553 or vehicle, at 45, 75, and 105 days after grafting. Bar, ± SEM. *, $P < 0.05$. **D,** tumor growth and migration analysis of GBM6-GFP-sh0 (a, b, e, f, i, and j) and GBM6-GFP-shEB1 (c, d, g, h, k, and l) cell lines injected in the SVZ of mice, treated (b, f, j, d, h, and l) or not (a, e, i, c, g and k) with BAL101553 at days 45, 75, and 105 after grafting. Serial sagittal sections show solid tumor and migrating tumor cells (GFP, green fluorescence). Bar, 250 μm. Three-dimensional reconstruction of brains is shown in each panel. Tumors (green), ventricles (blue), and corpus callosum (gray) are represented. Bar, 2.5 mm. (i), the inferior (left) and superior (right) views illustrate the strong invasivity of the tumor inside the brain.

BAL27862, active moiety of the prodrug BAL101553, nanomolar drug concentrations, inhibited growth of two glioblastoma CSLCs isolated from patients, that strikingly differ in their behavior and display molecular signatures specific for mesenchymal or proneural subtypes (GBM6 and GBM9, respectively). Interestingly, the antimigratory effect of BAL27862 was more pronounced in GBM6 cells that show a higher tumorigenicity with a more infiltrative pattern *in vivo*, and that strongly overexpress EB1 as compared with GBM9 (21–23). Consequently, we decided to fully investigate drug activity on GBM6 according to EB1 expression level, at subcytotoxic and cytotoxic concentrations *in vitro* and in orthotopically grafted mice. In control mice grafted with GBM6 sh0, administration of the prodrug BAL101553 enhanced survival and reduced tumor invasion inside the brain after only

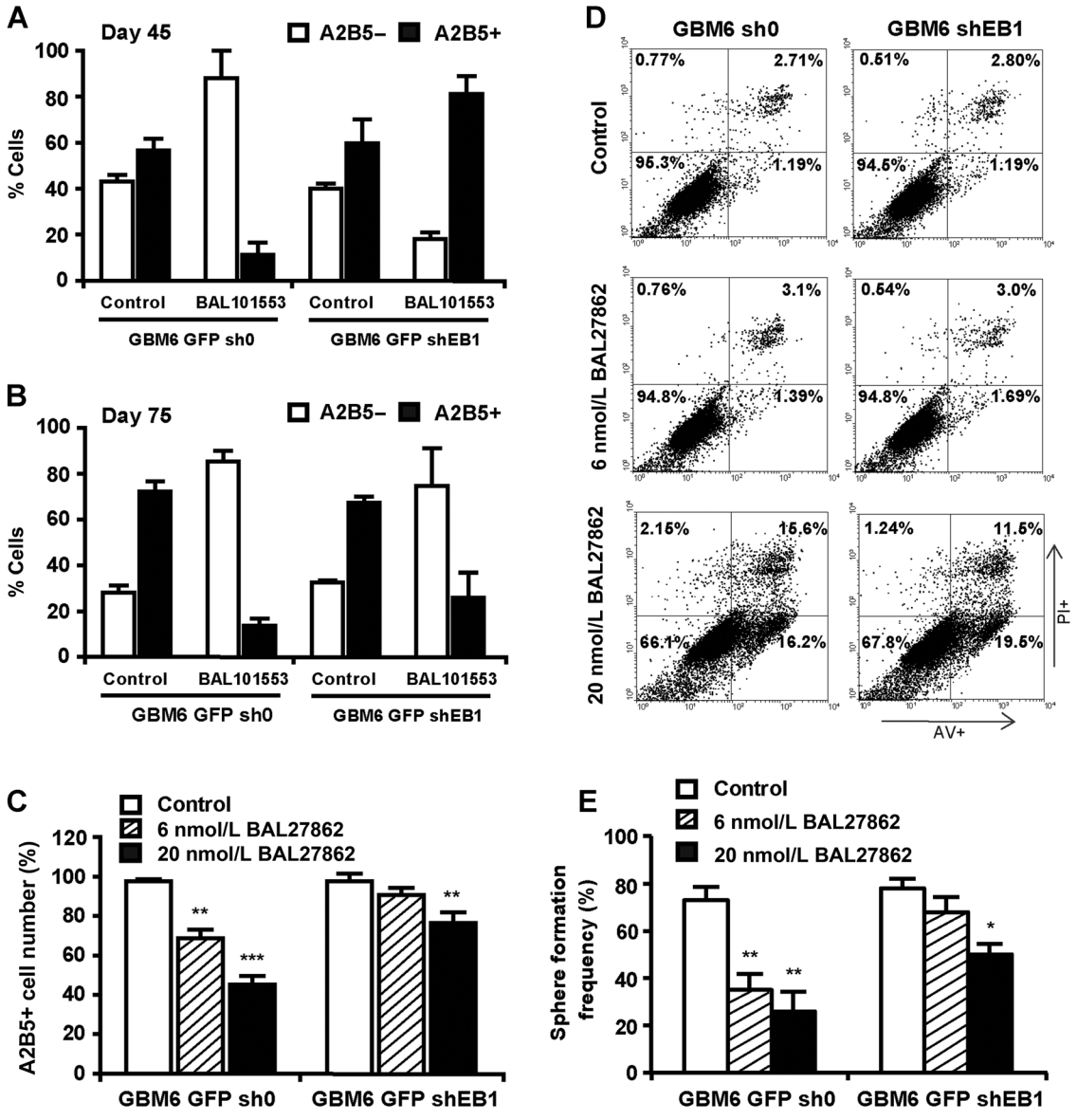

Figure 4.

BAL27862 induces loss of stem cell properties, potentiated by EB1 expression. **A** and **B,** quantification by FACS analysis of tumor cells isolated from brains of mice grafted with control GBM6-GFP-sh0 or GBM6-GFP-shEB1 treated with BAL101553 or vehicle, positive or not for A2B5 staining, at 45 (**A**) and 75 (**B**) days after grafting. **C,** quantification of GBM6-GFP-sh0 or GBM6-GFP-shEB1–positive cells for A2B5 staining treated or not with BAL27862 for 72 hours. **D,** characterization of cell death by FACS using annexin V and PI staining after BAL27862 treatment for 72 hours. Numbers in the quadrants indicate the mean of percentages of cells labeled with Annexin V–FITC (bottom right), PI (top left), Annexin V–FITC and PI (top right) and unlabeled (bottom left). **E,** quantification of the number of spheres. The percentage of sphere formation was calculated as the number of spheres formed divided by the original number of cells seeded. Bar, ± SEM. *, $P < 0.05$; **, $P < 0.005$, ***, $P < 0.001$.

three intravenous administrations over the course of a week. Indeed, tumor spreading remained confined around the site of injection, whereas it invaded the corpus callosum and deeper structures in vehicle-treated mice. Moreover, tumor growth was reduced by drug treatment, as shown by quantifying tumor cells in post-grafted brain. Importantly, BAL101553 also induced a loss of tumor stem cell properties *in vivo*, a phenomenon confirmed with BAL27862 *in vitro*. The self-renewal capacity and the proportion of $A2B5^+$ cells were decreased under treatment, without changing protein nor mRNA levels of the neuron-specific marker tubulin-βIII or the oligodendrocytic marker CNPase. On the contrary, the drug induced astroglial differentiation as shown by increased astrocyte-specific marker GFAP expression at both the mRNA and protein level. To our knowledge, BAL101553 is the first MTA that has demonstrated activity against CSLCs. As compared with currently approved MT stabilizing and depolymerizing agents, this novel small molecule has demonstrated several distinct effects on MT organization and dynamicity, with

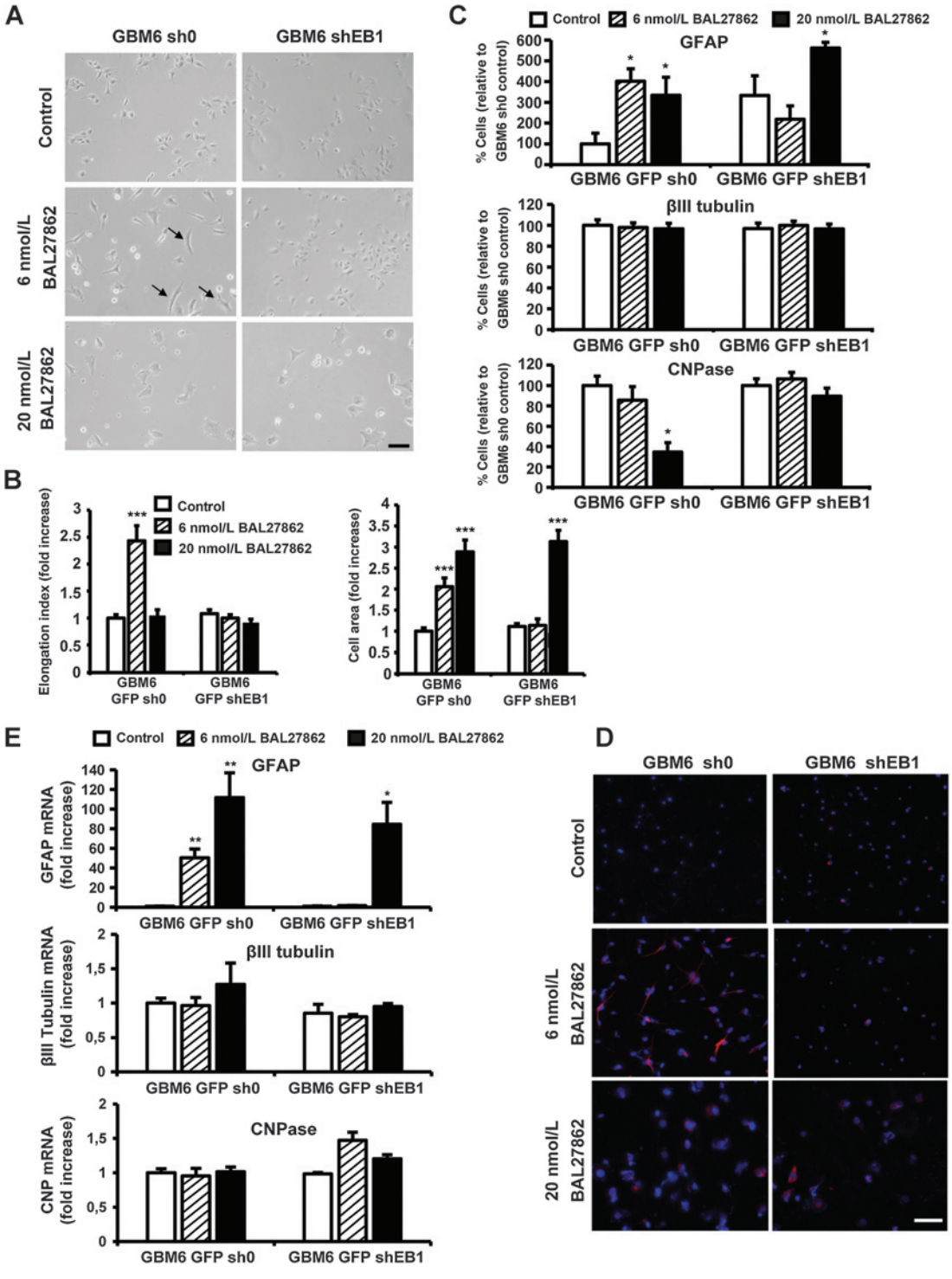

Figure 5.

BAL27862 induces GBM6 astrocytic differentiation, potentiated by EB1 expression. **A,** cell morphology was analyzed by phase-contrast microscope. Representative images of GBM6-GFP-shEB1 and control GBM6-GFP-sh0 cells treated or not (control) with BAL27862. Bar, 250 μm. **B,** fold increase in cell elongation index and cell area in the absence or presence of BAL27862. Cell elongation was quantified by measuring cell length and width and by calculating cell elongation index (length/width). Cell area was calculated using the formula (length × width × π)/4. **C,** BAL27862 triggers expression of GFAP astrocytic marker. GBM6-GFP-shEB1 and control GBM6-GFP-sh0 cells treated or not with BAL27862 for 72 hours. Cells were stained with GFAP, β-III-tubulin, or CNPase antibodies for FACS analysis. The percentage of GFAP, β-III-tubulin, and CNPase-positive cells is shown. **D,** cells were fixed and stained with anti-GFAP antibody and counterstained with DAPI. Bar, 500 μm. **E,** mRNA levels of GFAP, β-III-tubulin, or CNPase were analyzed by quantitative RT-PCR. *, $P < 0.05$; **, $P < 0.005$; ***, $P < 0.001$.

in vitro and *in vivo* activity against diverse human cancer models, including tumors refractory to conventional treatments (15). Moreover, in contrast to approved MTAs, which do not efficiently penetrate the brain, the promising pharmacokinetic properties of BAL101553 provide a strong rationale for its use for glioblastoma treatment. Indeed, the active drug has been shown to be efficiently distributed into the brain, with a 1:1 partitioning between plasma and brain tissue, no brain accumulation reported in rodent models (17) and currently no clinical indication of CNS toxicity in treated patients (19). With regard to activity on glioblastoma CSLCs, further work would be needed to determine whether this activity is shared by other MTAs.

Our results highlight both EB1-independent and EB1-dependent effects of BAL101553. Indeed, EB1-independent effects consist of induction of apoptosis and cytotoxicity at high concentrations, which are the classical effects described for MTAs. In contrast, the EB1-dependent effect observed only in glioblastoma CSLCs overexpressing EB1 (17× in comparison with U87-MG cells) at subcytotoxic concentrations consists of an antimigratory activity, inhibition of self-renewal, anticlonogenicity, and astrocytic differentiation. These results support EB1 expression to be of predictive value for BAL101553 response in glioblastoma patients. The current study also provides new data on the role of EB1 in glioblastoma progression. The promigratory and proinvasive roles of EB1, as well as the poor survival associated with high levels of EB1 previously shown in glioblastoma cells overexpressing EB1, are now extended to glioblastoma CSLCs. Interestingly, the low level of GFAP protein expression in control cells suggests that EB1 is also involved in maintaining a low level of differentiation in such invasive cells. Together, these data strengthen the bad prognostic value of EB1 overexpression in glioblastoma and its predictive role in MTA response, as we previously mentioned for *vinca*-alkaloids (21).

All these results suggest that MT dynamics plays a crucial role in glioblastoma progression and MTA response. Interestingly, the MT-associated protein doublecortin, that shares its binding site with EB1 at MT + ends but with a different mechanism of binding (26), has also been found overexpressed in invasive human brain tumors (27) with bad prognosis (28). This is consistent, with our previous evaluation of EB1 in a large cohort of glioblastoma patients (21). The mechanism of sensitization to MTAs by EB1 is most likely related to their effects on MT dynamics as demonstrated *in vitro* (29, 30) and in U87-MG glioblastoma cells for vincristine and BAL27862 (21). Importantly, the amount of EB1 strongly influences the way MT dynamic instability is altered, and post-translational modifications of EB1 also modulate the regulation of MT dynamics, proliferation/migration, or MTA response (31, 32). Moreover, MT organization and dynamic properties change as cells differentiate, forming a more parallel MT array with fast and persistent growth excursions (33). Several studies have shown that differentiation of CSLCs is not a one-way route but might be a reversible process that can be directed by signals from the tumor microenvironment (34–35), including endothelial cells (36, 37). Interestingly, we recently demonstrated that the MT cytoskeleton is able to adapt its dynamic properties according to extracellular stimuli such as vascular endothelial growth factor, a process in which EB1 detyrosination plays a crucial role (31). One hypothesis concerning the effect of BAL101553 on CSLCs differentiation is that the drug by affecting MT dynamics may disrupt an extracellular and/or intracellular signal leading to a de-differentiation pathway.

The loss of stemness may be an important mechanism possibly leading to sensitization of gliomas to other therapies or inhibiting the emergence of therapy-resistant tumor cell clones. However, recent demonstration of de-differentiation of glioblastoma cell lines into CSLCs proves that any successful therapeutic agent or combination of drugs for glioblastoma therapy must eliminate not only CSLCs but also the differentiated glioblastoma cells and the entire bulk of tumor cells (38, 39). In this context, we have shown that BAL101553 does exert the classical cytotoxic activity associated with MTAs by inducing apoptosis in glioblastoma CSLCs, similar to previous observations in glioblastoma tumor cell lines (17). However, the drug also displays another characteristic, characterized by a strong inhibition of glioblastoma CSLC migration associated with a loss of stem cell properties and differentiation toward the astrocytic route. These data, therefore, support the hypothesis that microtubule targeting as an approach for glioblastoma treatment could fulfill the requirement of targeting both tumor cell and CSLC compartments in order to achieve maximal clinical benefit. Moreover, subcytotoxic drug levels may be sufficient to achieve the latter. Together with the potential use of EB1 expression as a biomarker predictive of drug sensitivity, these data support the development of novel MTAs, such as BAL101553, for the management of aggressive EB1-overexpressing glioblastomas.

Disclosure of Potential Conflicts of Interest

F. Bachmann has ownership interest in stock options of Basilea Pharmaceutica H.A. No potential conflicts of interest were disclosed by the other authors.

Authors' Contributions

Conception and design: R. Bergès, S. Honoré, F. Bachmann, H.A. Lane, D. Braguer

Development of methodology: R. Bergès, A. Tchoghandjian, D. Figarella-Branger, F. Bachmann

Acquisition of data (provided animals, acquired and managed patients, provided facilities, etc.): R. Bergès, A. Tchoghandjian, D. Figarella-Branger

Analysis and interpretation of data (e.g., statistical analysis, biostatistics, computational analysis): R. Bergès, A. Tchoghandjian, S. Honoré, D. Figarella-Branger, F. Bachmann, H.A. Lane, D. Braguer

Writing, review, and/or revision of the manuscript: R. Bergès, A. Tchoghandjian, S. Honoré, M.-A. Estève, D. Figarella-Branger, F. Bachmann, H.A. Lane, D. Braguer

Administrative, technical, or material support (i.e., reporting or organizing data, constructing databases): R. Bergès, F. Bachmann

Study supervision: R. Bergès, D. Braguer

Acknowledgments

This work has been carried out thanks to the support of the A*MIDEX project (No. ANR-11-IDEX-0001-02) funded by the "Investissements d'Avenir" French Government program, managed by the ANR, DGOS (SIRIC label) INCa-DGOS-Inserm no. 6038, the ITMO Cancer AVIESAN as part of the Cancer Plan no. PC201419, and Basilea Pharmaceutica International Ltd. The authors wish to thank Dr. N. Baeza-Kallee, H. Gallardo, and Caroline Schläfle for technical help and E. Lopez from the CFREMC (Centre de Formation et de Recherches Expérimentales Médico-Chirurgicales, numéro d'agrément: E 13-055-5), 13385 Marseille, France.

Grant Support

This was supported by the A*MIDEX project (No. ANR-11-IDEX-0001-02) funded by the "Investissements d'Avenir" French Government program,

managed by the ANR (D. Braguer and S. Honoré), DGOS (SIRIC label) INCa-DGOS-Inserm no. 6038 (D. Figarella-Branger), the ITMO Cancer AVIESAN as part of the Cancer Plan no. PC201419 (S. Honoré), Basilea Pharmaceutica International Ltd (H.A. Lane and F. Bachmann).

The costs of publication of this article were defrayed in part by the payment of page charges. This article must therefore be hereby marked *advertisement* in accordance with 18 U.S.C. Section 1734 solely to indicate this fact.

Received April 25, 2016; revised July 25, 2016; accepted August 9, 2016; published OnlineFirst August 18, 2016.

References

1. Louis DN, Ohgaki H, Wiestler OD, Cavenee WK, Burger PC, Jouvet A, et al. The 2007 WHO classification of tumours of the central nervous system. Acta Neuropathol 2007;114:97–109.
2. Giese A, Bjerkvig R, Berens ME, Westphal M. Cost of migration: invasion of malignant gliomas and implications for treatment. J Clin Oncol 2003;21: 1624–36.
3. Charles NA, Holland EC, Gilbertson R, Glass R, Kettenmann H. The brain tumor microenvironment. Glia 2011;59:1169–80.
4. Binello E, Germano IM. Targeting glioma stem cells: a novel framework for brain tumors. Cancer Sci 2011;102:1958–66.
5. Cheng L, Bao S, Rich JN. Potential therapeutic implications of cancer stem cells in glioblastoma. Biochem Pharmacol 2010;80:654–65.
6. Tabatabai G, Weller M. Glioblastoma stem cells. Cell Tissue Res 2011;343: 459–65.
7. Venere M, Fine HA, Dirks PB, Rich JN. Cancer stem cells in gliomas: identifying and understanding the apex cell in cancer's hierarchy. Glia 2011;59:1148–54.
8. Ortensi B. Cancer stem cell contribution to glioblastoma invasiveness. Stem Cell Res Thera 2013;4:18.
9. Jordan MA, Wilson L. Microtubules as a target for anticancer drugs. Nat Rev Cancer 2004;4:253–65.
10. Kavallaris M. Microtubules and resistance to tubulin-binding agents. Nat Rev Cancer 2010;10:194–204.
11. Nathanson D, Mischel PS. Charting the course across the blood–brain barrier. J Clin Invest 2011;121:31–3.
12. Prota AE, Danel F, Bachmann F, Bargsten K, Buey RM, Pohlmann J, et al. The novel microtubule-destabilizing drug BAL27862 binds to the colchicine site of tubulin with distinct effects on microtubule organization. J Mol Biol 2014;426:1848–60.
13. Rovini A, Honore S, McKay N, Bachmann F, Lane HA, Braguer D. Antitumor activity of BAL27862 (active moiety of the prodrug BAL101553) is associated with the generation of short non-centrosomal microtubules. Eur J Cancer 2012;48:abstract 422.
14. Bachman F, Burger K, Lane HA. BAL101553 (prodrug of BAL27862): the spindle assembly checkpoint is required for anticancer activity Cancer Res 2015;75:abstract 3789.
15. Duran GE, Lane H, Bachmann F, Sikic BI. In vitro activity of the novel tubulin active agent BAL27862 in MDR1(+) and MDR1(–) human breast and ovarian cancer variants selected for resistance to taxanes. Cancer Res 2010;70:abstract 4412.
16. Esteve MA, Honore S, McKay N, Bachmann F, Lane H, Braguer D. BAL27862: a unique microtubule-targeted drug that suppresses microtubule dynamics, severs microtubules, and overcomes Bcl-2- and tubulin subtype-related drug resistance. Cancer Res 2010;70:abstract 1977.
17. Schmitt-Hoffmann A, Klauer D, Gebhardt K, Fullhardt P, Brendle A, Hardgreaves P. BAL27862: A unique microtubule-targeted agent with a potential for the treatment of human brain tumors. Mol Cancer Ther 2009;8:abstract C233.
18. Pohlmann J, Bachmann F, Schmitt-Hoffmann A, Biringer G, Burger K, Bucher C, et al. BAL101553: A highly soluble prodrug of the potent microtubule destabilizer BAL27862. Cancer Res 2010;70: abstract 4419.
19. Lopez J, Jeffry Evans TR, Plummer ER, Diamantis N, Shaw HM, Zubairi IH, et al. Phase 1/2a trial of intravenous BAL101553, a novel tumor checkpoint controller (TCC), in advanced solid tumors. ASCO (American Society of Clinical Oncology) meeting 2016; Abstract 2525.
20. Kristeleit RS, Jeffry Evans TR, Lopez J, Slater S, D'Arcangelo M, Drew Y, et al. A Phase 1 study to assess the safety, pharmacokinetics (PK), pharmacodynamics (PD) and antitumor activities of daily oral BAL101553, a novel tumor checkpoint controller (TCC) in adult patients with advanced solid tumors. ASCO (American Society of Clinical Oncology) meeting 2016; Abstract TPS2594.
21. Berges R, Baeza-Kallee N, Tabouret E, Chinot O, Petit M, Kruczynski A, et al. End-binding 1 protein overexpression correlates with glioblastoma progression and sensitizes to Vinca-alkaloids in vitro and in vivo. Oncotarget 2014;5:12769–87.
22. Tchoghandjian A, Baeza N, Colin C, Cayre M, Metellus P, Beclin C, et al. A2B5 cells from human glioblastoma have cancer stem cell properties. Brain Pathol 2010;20:211–21.
23. Tchoghandjian A, Baeza-Kallee N, Beclin C, Metellus P, Colin C, Ducray F, et al. Cortical and subventricular zone glioblastoma-derived stem-like cells display different molecular profiles and differential in vitro and in vivo properties. Ann Surg Oncol 2012;19:S608–19.
24. Denicolai E, Baeza-Kallee N, Tchoghandjian A, Carre M, Colin Jiglaire CJ, et al. Proscillaridin A is cytotoxic for glioblastoma cell lines and controls tumor xenograft growth in vivo. Oncotarget 2014;5:10934–48.
25. Schroeder A, Mueller O, Stocker S, Salowsky R, Leiber M, Gassmann M, et al. The RIN: an RNA integrity number for assigning integrity values to RNA measurements. BMC Mol Biol 2006;7:3.
26. Bechstedt S, Lu K, Brouhard GJ. Doublecortin recognizes the longitudinal curvature of the microtubule end and lattice. Curr Biol 2014;24:2366–75.
27. Daou MC1, Smith TW, Litofsky NS, Hsieh CC, Ross AH. Doublecortin is preferentially expressed in invasive human brain tumors. Acta Neuropathol 2005;110:472–80.
28. Rich JN, Hans C, Jones B, Iversen ES, McLendon RE, Rasheed BK. Gene expression profiling and genetic markers in glioblastoma survival. Cancer Res 2005;65:4051–8.
29. Mohan R, Katrukha EA, Doodhi H, Smal I, Meijering E, Kapitein LC, et al. End-binding proteins sensitize microtubules to the action of microtubule-targeting agents. Proc Natl Acad Sci U S A 2013;110:8900–905.
30. Pagano A, Honore S, Mohan R, Berges R, Akhmanova A, Braguer D. Epothilone B inhibits migration of glioblastoma cells by inducing microtubule catastrophes and affecting EB1 accumulation at microtubule plus ends. Biochem Pharmacol 2012;84:432–43.
31. Rovini A, Gauthier G, Berges R, Kruczynski A, Braguer D, Honore S. Antimigratory effect of vinflunine in endothelial and glioblastoma cells is associated with changes in EB1 C-terminal detyrosinated/tyrosinated status. PLoS One 2013;8:e65694.
32. Le Grand M, Rovini A, Bourgarel-Rey V, Honore S, Bastonero S, Braguer D, et al. ROS-mediated EB1 phosphorylation through Akt/GSK3β pathway: implication in cancer cell response to microtubule-targeting agents. Oncotarget 2014;5:3408–23.
33. Lacroix B, Maddox AS. Microtubule dynamics followed through cell differentiation and tissue biogenesis in C. elegans. Worm 2014;3:e967611.
34. Vermeulen L, De Sousa EMelo F, van der Heijden M, Cameron K, de Jong JH, et al. Wnt activity defines colon cancer stem cells and is regulated by the microenvironment. Nat Cell Biol 2010;12:468–76.
35. Vermeulen L, de Sousa e Melo F, Richel DJ, Medema JP. The developing cancer stem-cell model: clinical challenges and opportunities. Lancet Oncol 2012;13:e83–9.
36. Fessler E, Dijkgraaf FE, De Sousa E Melo F, Medema JP. Cancer stem cell dynamics in tumor progression and metastasis: is the microenvironment to blame? Cancer Lett 2013;341:97–104.
37. Fessler E, Borovski T, Medema JP. Endothelial cells induce cancer stem cell features in differentiated glioblastoma cells via bFGF. Mol Cancer 2015; 14:157.
38. Liu Y, Ye F, Yamada K, Tso JL, Zhang Y, Nguyen DH. Autocrine endothelin-3/endothelin receptor B signaling maintains cellular and molecular properties of glioblastoma stem cells. Mol Cancer Res 2011;12:1668–85.
39. Olmez I, Shen W, McDonald H, Ozpolat B. Dedifferentiation of patient-derived glioblastoma multiforme cell lines results in a cancer stem cell-like state with mitogen-independent growth. J Cell Mol Med 2015;19: 1262–972.